Article

Prospects of Intraoperative Multimodal OCT Application in Patients with Acute Mesenteric Ischemia

Elena Kiseleva [1,*], Maxim Ryabkov [2], Mikhail Baleev [3], Evgeniya Bederina [2], Pavel Shilyagin [4], Vladimir Beschastnov [3], Ivan Romanov [3], Grigory Gelikonov [4] and Natalia Gladkova [1]

[1] Institute of Experimental Oncology and Biomedical Technologies, Privolzhsky Research Medical University, 10/1 Minin and Pozharsky Sq., 603950 Nizhny Novgorod, Russia; kiseleva84@gmail.com (E.K.); natalia.glad-kova@gmail.com (N.G.)

[2] University Clinic, Privolzhsky Research Medical University, 18/1 Verkhnevolzhskaya naberezhnaja, 603155 Nizhny Novgorod, Russia; maxim-ryabkov@yandex.ru (M.R.); genacrok@gmail.com (E.B.)

[3] City Clinical Hospital No.30, 85A Berezovskaya St., 605157 Nizhny Novgorod, Russia; mihaboks@mail.ru (M.B.); vvb748@mail.ru (V.B.); post@hospital30.ru (I.R.)

[3] Institute of Applied Physics of the RAS, 46 Ulyanova St., 603950 Nizhny Novgorod, Russia; paulo-s@mail.ru (P.Sh.); grgel@yahoo.com (G.G.)

[*] Correspondence: e kiseleva84@gmail.com; Tel.: +7-920-059-0536

Abstract: Introduction: Despite the introduction of increasingly multifaceted diagnostic techniques and the general progress of emergency abdominal and vascular surgery, the outcome of treatment of patients with acute impaired intestinal circulation remains unsatisfactory. The non-invasive and high-resolution technique of optical coherence tomography (OCT) can be used intraoperatively to assess intestine viability and associated conditions that frequently emerge under conditions of impaired blood circulation. This study aims to demonstrate the effectiveness of multimodal (MM) OCT for intraoperative diagnostics of both the microstructure (cross-polarization OCT mode) and microcirculation (OCT angiography mode) of the small intestine wall in patients with acute mesenteric ischemia (AMI). Methods and Participants: A total of 18 patients were enrolled in the study. Nine of them suffered from AMI in segments II-III of the superior mesenteric artery (AMI group), where the ischemic segments of the intestine were examined. Nine others were operated for adenocarcinoma of the colon (control group), thus allowing areas of their normal small intestine to be examined for comparison. Data on the microstructure and microcirculation in the walls of the small intestine were obtained intraoperatively from the side of the serous membrane using the MM OCT system (IAP RAS, Russia) before bowel resection. The MM OCT data were compared with the results of histological examination. Results: The study finds that MM OCT visualized the damage to serosa, muscularis externa, and blood vessels localized in these layers in 100% of AMI cases. It also visualized the submucosa in 33.3% of AMI cases. The MM OCT image of non-ischemic (control group), viable ischemic and necrotic small intestines (AMI group) differed significantly across stratification of the distinguishable layers, the severity of intermuscular fluid accumulations and the type and density of the vasculature. Conclusion: The MM OCT diagnostic procedure optimally meets the requirements of emergency surgery. Data on the microstructure and microcirculation of the intestinal wall can be obtained simultaneously in real time without requiring contrast agent injections. The depth of visualization of the intestinal wall from the side of the serous membrane is sufficient to assess the volume of the affected tissues. However, the methodology for obtaining MM OCT data needs to be improved to minimize the motion artefacts generated in actual clinical conditions.

Keywords: Keywords: acute mesenteric ischemia (AMI); optical coherence tomography (OCT); optical coherence angiography (OCA); intraoperative diagnostics; gut vitality; image assessment

1. Introduction

Acute mesenteric ischemia (AMI) is a sudden interruption of the blood supply to a segment of the small intestine leading to ischemia, cellular damage, intestinal necrosis, and eventually patient death if left untreated [1]. The disease accounts for approximately 0.2% of emergency hospital admissions [2] even though over the past year the incidence has increased among adults [3–5] and children [6] due to the spread of COVID-19 infection.

AMI is life threatening for patients and a challenge for clinicians. Despite the introduction of increasingly advanced methods of diagnosis and treatment, the AMI mortality rate remains very high (45-85%) [7]. In most patients, ischemia would have lasted for more than 12 hours prior to surgical intervention. Therefore, it is expected that large areas of necrosis would appear in the intestine. However, as the peripheral areas of the ischemic intestine continue to be partially supplied with blood from the collateral vessels, the damage is likely to be heterogeneous. One of the unresolved clinical quandaries is the objectivity of the intraoperative assessment of the viable sections of the intestine. Verification of regions of impaired blood circulation and tissue necrosis is essential for the selection of boundaries for bowel resection. Accurate verification reduces the risk of anastomotic leakage and helps prevent post-resection indigestion [8].

Currently, there are limited intraoperative tools available to surgeons while deciding on bowel viability. Surgeons mainly rely on a subjective assessment of the color and mobility of the intestine, and the presence of blood vessels pulsation. Thus, it is impossible to adequately assess the degree of ischemia-induced changes inside the intestinal wall. Studies on clinical estimation of bowel viability report an overall accuracy of 89% (positive predictive value 64%). In 46% of the cases, unnecessary bowel resection was reported [9]. Leaving non-viable intestine can lead to sepsis [10,11], while extensive resection of bowel can lead to short-bowel syndrome [12].

Various optical technologies could be used, allowing for direct visualization or quantification of the prevalence and severity of intestinal ischemia based on the intraoperative evaluation of microcirculation. These tools include Laser Doppler Flowmetry (LDF) and fluorescence imaging (FI). The former method is one of the pioneers of gut perfusion assessment [13–17], whereas the latter is widely used in contemporary clinical practice [18–21]. Note that, the use of LDF has not become widespread in AMI affected patients, even though the method continues to be of interest in experimental studies of intestinal tissue damage after ischemia/reperfusion injury [22,23]. The last two years have witnessed an increase in the usage of LDF in combination with visible light spectroscopy in the gastroscopy of patients with chronic mesenteric ischemia [24,25]. A number of research groups expressed optimism regarding the great potential of FI using indocyanine green dye for routine use [19,20,26]. FI reduces operation time and the technique has a laparoscopic potential. Even though FI is currently a method of choice in AMI, it is still not formally accepted as the standard of clinical care for intraoperative assessment of bowel viability [2,27]. Some researchers have found that FI is more useful than other available methods [19,20], whereas others have shown its low significance [9,28,29].

Other optical methods that demonstrate potential in the detection of perfusion changes in the gut includes sidestream dark field (SDF) microscopy [30–32], incident dark field (IDF) imaging [33,34] and hyperspectral imaging (HSI) [35]. SDF and IDF are a non-invasive microscopy for quantitative perfusion imaging, but have not been used in AMI. SDF demonstrate potential in the evaluation of perfusion of gastric tube [32] and colon [30,31] so that a reduction in anastomotic leakage could be accomplished. IDF with quantification related perfusion parameters was used in [33] only to determine angioarchitecture of the peritoneum, including capillaries. HSI is a novel technique for applications in intestinal ischemia. During a HSI imaging false-color-images that represent different parameters of tissue oxygenation are generated [36]. [35] demonstrates that HSI is able to discriminate tissue perfusion in AMI reliably and therefore might be helpful for resection.

However, a more convincing assessment of the utility of HSI in AMI would require a cohort study with longitudinal and structured data.

Laser speckle contrast imaging (LSCI) is also a prospective technique for intraoperative assessment of intra-abdominal microcirculation in AMI [37,38]. However, so far it was only used for the identification of ischemic areas on gastric tube reconstructions [39,40] and during colorectal surgery [41]. It is noteworthy that a special laparoscopic vision system integrating LSCI with a commercially available rigid laparoscope has already been developed and tested [42].

The abovementioned methods have their own advantages and limitations [43–45]. Furthermore, the intestine as an extraordinarily mobile research object also imposes additional constraints on the imaging tools and methods in terms of frequency, quality and repeatability of the collected data. In particular, difficulties are caused by point research (LDF, SDF, IDF,) or non-contact (SDF, IDF, HIS, LSCI) methods.

Unfortunately, all of the above methods evaluate only intestinal perfusion and flowmetry, and ignore the assessment of structural tissue damage or the direct presence of necrosis.

Optical coherence tomography (OCT) angiography is a multimodal technology for the simultaneous visualization of the structure and microcirculation of the studied organ and is most effectively used in ophthalmology [46]. Thus, it is a promising tool for the complex assessment of the intestinal wall damage caused by AMI. The experience of experimental and clinical application of OCT in gastroenterology indicates the possibility of the label-free imaging of the gut wall stratification with the resolution of 25 microns or less to the depth of 2 mm [47–49]. In the overwhelming majority of clinical studies using OCT, the gastrointestinal tract visualization has been carried out by endoscopic access, which has facilitated the assessment of mucous membranes of esophagus [50], stomach [51], the initial part of small intestine and colon [52,53]. The main purpose of this procedure is to detect dysplastic epithelium, neoplasms and to clarify the boundaries of tumor growth using only structural OCT images [54,55], or in combination with analysis of the mucosal microcirculation [54,56]. Methods are being developed for multivariate quantitative analysis of structural OCT images obtained from *ex vivo* gastric and intestinal samples of the mucous membranes to make possible the use of such imaging of *in vivo* tissues for clinical applications in the future [57].

Due to the limited length of available probes for endoscopic intraluminal OCT, the small intestine distal to the duodenum and proximal to the cecum is still the least studied segment of the digestive tract using OCT [48]. A trans-serous transabdominal approach to an OCT study in a clinic would remove these restrictions and enable visualization of the serous and muscular membranes, and the network of subserous and submucous blood vessels in any segment of the small intestine. This is very important for diagnosing the prevalence of AMI. In [58], OCT was used to determine the degree of perfusion of the anastomosis of the esophagus by the stomach wall during reconstructive surgery. However, it used OCT from the outer layer of the gastrointestinal tract. An OCT picture of ischemic damage to the wall of the small intestine in humans with AMI has not been previously obtained or assessed. We set out to test whether multimodal (MM) OCT, which has proven its effectiveness in studies on AMI models in laboratory animals [49,59]. This would enable us to obtain objective data on the state of the human intestinal wall with AMI in a clinical situation.

The purpose of this study is to demonstrate the effectiveness and prospects of transserous MM OCT in intraoperative diagnosis of the microstructure and microcirculation of the small intestine wall in patients with AMI.

2. Materials and Methods

2.1. Preparatory Animal Study

Porcine intestine was selected for the testing and probe positioning during MM OCT imaging. In terms of structure and thickness of the wall, this is nearest to the intestines of

our human experimental subjects. It is known that many physiological movements of the gut and of the organism as a whole can lead to significant artefacts in the OCT data. Therefore, the stabilization of the probe and the object under study is critical for obtaining high-quality structural OCT, and especially, OCA images.

Normal small intestine of a laboratory miniature pig was imaged with MM OCT before the clinical study. One Wiesenau male miniature pig, 4 months old, weighing 37 kg was used. The animal was kept in accordance with the rules adopted by the European Convention for the Protection of Vertebrate Animals used for Experimental and Other Scientific Purposes (Strasbourg, 1986). The small intestine was accessed through a layered midline laparotomy under combined (gas and intravenous) anesthesia, with continuous monitoring of the electrocardiogram, blood pressure, and body temperature.

2.2. Patients

The controlled single-center observational study included 18 patients (10 men and 8 women). All of them were operated in 2019–2020 for their abdominal surgical pathology. Target group included 9 patients who were hospitalized and urgently operated for AMI. Inclusion criteria: AMI as a result of thrombosis; embolism of arteries associated with segments II–III of the superior mesenteric artery with acute ischemia of the ileum. Exclusion criteria: thrombosis or embolism in segment I of the superior mesenteric artery; the use of vasopressors in the perioperative period to relieve hypotension. The diagnosis of AMI in 5 out of the 9 patients was established before laparotomy on the basis of the clinical picture and computed tomography data, while in the other 4 patients: in 2 cases on the basis of the clinical picture and diagnostic laparoscopy data, and in the remaining 2 cases the diagnosis was made only after an emergency laparotomy performed because of a clinical picture of acute surgical abdomen of unknown etiology. The volume of surgery in target group involved resection of a non-viable part of the small intestine, the boundaries of which were determined by visual-palpation criteria [2]. Control group included 9 patients who were on planned treatment for adenocarcinoma of the colon (T3-4N0M0), without intestinal obstruction, bleeding, perforation or other intra-abdominal complications. The scope of the operation in this group was right-sided hemicolectomy with resection of the terminal section of the ileum. Since the blood supply and structure of the ileal section in these patients were not impaired in any way (the distance from the tumor was more than 60 cm), the parameters of the wall of this section of the intestine were diagnosed as normal. In terms of gender, age, frequency and spectrum of comorbidities, patients in the study groups did not differ statistically significantly (in all cases $p > 0.5$) (Table 1).

Table 1. Characteristics of the patient groups.

| Characteristic	AMI Group	Control group
Sex (male/famele), n	6/3	4/5
Median age, years, Me [Q1;Q3]	67 [62; 73]	62 [57; 69]
Median body mass index, Me [Q1;Q3]	24,8 [23,4; 26,8]	27,3 [26,2; 27,7]
Smoker, n	3	2
Diabetes, n	1	2
Hypertension, n	6	5
Chronic obstructive pulmonary disease, n	1	0

Preoperative and postoperative therapies and surgical interventions were performed in accordance with the established protocols and standards of medical care [2]. The study was carried out in accordance with international ethical principles and the regulatory requirements of Russian Federation. All patients received an exhaustive explanation of the purpose, algorithm, and possible consequences of intraoperative therapeutic and diagnostic manipulations, after which they gave informed consent for the procedures to be performed to carry them out. This study was approved by the review board of the Privolzhsky Research Medical University (Protocol #17 from 10 November 2019). The

research was carried out within the framework of the RSF project #19-75-10096, agreement 19-75-10096 from 09 August 2019.

2.3. MM OCT device

A custom-made spectral-domain MM OCT setup (Figure 1b) was used in the study (Institute of Applied Physics of the RAS, Russia) [60] for contact intraoperative visualization of the intestinal walls of the patients (Figure 1a,c). The setup combines traditional structural OCT as well as cross-polarization and angiography modes [61].
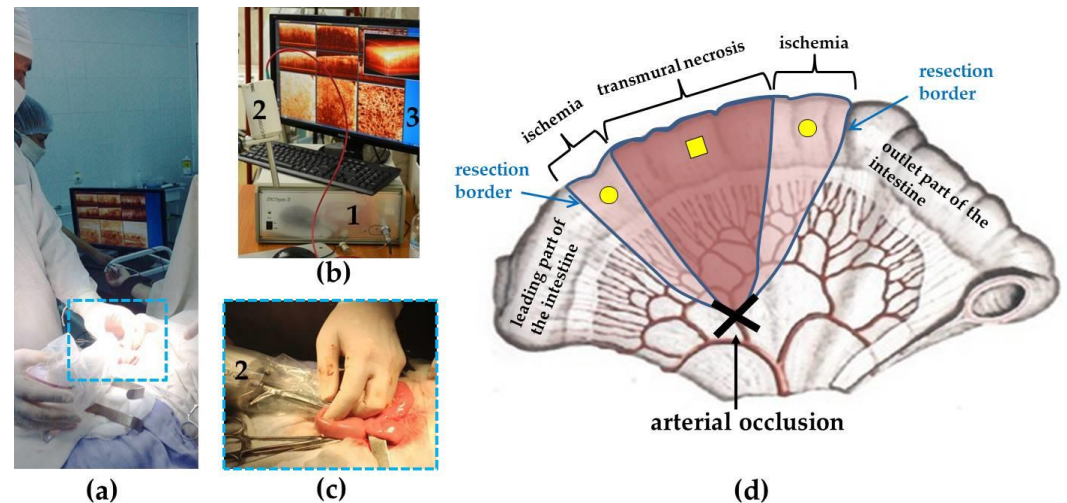
Figure 1. The procedure for intraoperative small intestine visualization using MM OCT. (**a**) general overview of the trans-serous MM OCT study; (**b**) MM OCT system (1) with probe (2) and an example of data set acquired after tissue scanning (3); (**c**) the probe (2) in a sterile sheath is installed on the surface of the normal ileum; (**d**) diagram of the MM OCT study of ischemic bowel: square mark — point of the OCT probe localization on the anesthetized part of the intestine, round marks — points from which MM OCT images were obtained from the ischemic areas of the intestine to be resected.

The radiation source in the device is a superluminescent diode with a central wavelength of 1310 nm. The longitudinal resolution is 10 μm and the lateral resolution 15 μm, while, the scanning depth in air is ~ 1.7 mm, and the scanning rate is 20,000 A-scans per second. Continuous 2D scanning is performed along the fast axis (512 spectral measurements, 256 spectral A-scans) and along the slow axis (1024 B-scans), which are summed in a 3D image (Figure 2c, Figure 3c, Figure 4c, Figure 5c). As a result, 2D depth-wise images (Figure 2b,e; Figure 3b,e; Figure 4b,e; Figure 5b,e) and en-face images (Figure 2a,d; Figure 3a,d; Figure 4a,d; Figure 5a,d) are available for display and evaluation. The use of circularly polarized light allows for the construction of two types of structural images. The first image type reflects the degree of backscattering of light from all those tissue components capable of backscattering probe radiation (image in co-polarization) (Figure 2a, Figure 3a,b; Figure 4a,b; Figure 5a,b), whereas the second image type shows the result of only the cross-scattering from fibrous components (mainly collagen, and to a lesser extent from muscle fibers), when the initial orientation of the polarization vector of the probe radiation changes to orthogonal (image in cross-polarization) (Figure 2d,e; Figure 3d,e; Figure 4d,e; Figure 5d,e). Both images are combined into one cross-polarization (CP) OCT image.

The vascular imaging includes an en-face optical coherence angiography (OCA) image (Figure 2g, Figure 6) constructed during the process of data acquisition. This occurs after applying a high-pass filter (filter cutoff at 96 Hz) to the recorded data along the slow axis. With this filtering parameter, areas where blood flow is occurring are visualized. Places where blood is in a stationary state are not visualized. For OCT angiographic analysis, each obtained 3D microvascular network was converted to 2D image with Maximum Intensity Projection (MIP) by projecting the desired imaged depth onto the plane. The

OCA images shown in the study were not post-processed to remove motion artefacts, as the purpose of using OCA for microvascular network visualization in the intestines of patients in this study was to demonstrate the applicability of the method to real clinical conditions, rather than to present a scrupulous quantitative assessment of the vascular network.

It takes 26 seconds to acquire one set of images. This includes a 3D image, 2D depth-wise images in different planes, 2D en-face images, and an OCA image of the intestine (Figure 1b, number 3).

As a design feature, the MM OCT device included an elongated cylindrical contact probe 15 cm long and 1 cm in diameter (Figure 1b, number 2). In an open operation with a laparotomic approach, such a probe design provided visualization in all cases of the small intestine segments requiring to be examined. During scanning, the probe was held either in the surgeon's hand, or was rigidly fixed onto a special holder (KARL STORZ SE & Co. KG, Germany).

2.4. MM OCT Examination of the Small Intestine

MM OCT data were obtained by trans-serous access during laparotomy (in porcine) and surgery (in patients). The optical probe was placed in contact with the lateral surface of the intestine, at a point equidistant from the mesenteric and antimesenteric edges (Figure 1d).

For the porcine tests, twelve 3D MM OCT images were obtained from the small intestine of the pig: 3 volumetric images were recorded from each of the four zones of the intestine to be taken for histological examination.

In the studied groups of patients, a total of 60 3D images were obtained, 45 of which with the least number of artefacts were selected for further analysis. In AMI group, a total number of 3D images was 27 and they were obtained from three locations. One of these locations was in the center of the affected segment, where the intestine had a cyanotic color, there was no shine to the peritoneum, the mesenteric vessels did not pulsate and there was no observable peristalsis. 9 volumetric images were reordered from this point. The other two locations (18 volumetric images) — at the periphery of the ischemic area (left and right), where the color and luster of the intestine were changed and peristalsis was weakened, but where there were no visual signs of transmural necrosis (Figure 1d). These parts of the intestine also had to be removed. Thus, all 27 areas of the MM OCT study were within the resection and were subject to subsequent histological confirmation. In the control group prior to hemicolectomy, 18 3D datasets were obtained from 2 locations of the normal ileum: at the proposed border of resection for the possibility of comparison with histological data, and at a point located 25 ± 2 cm proximal to the ileocecal angle — from the zone corresponding to a similar area in the case of the ischemic small intestine. No histological verification of this section of the small intestine was required due to the similarity in the histological structure of the two studied areas of the control group.

For the assessment of structural CP OCT images from each sampled volume several (2-4) representative 2D cross-sectional and 2D en-face images at the depth of different intestinal wall layers were saved and assessed. In terminology, cross-sectional CP OCT images will be called B-scans, as is customary in OCT technology [62]. During visual analysis of the CP OCT images, two characteristics of the intestinal wall microstructure were assessed: 1) the number of intestinal wall layers that could be differentiated on the B-scans; 2) the presence and severity of signs of intermuscular edema — this sign was assessed both in the B-scans and in the en-face images.

Microcirculation was analyzed in 2D en-face OCA images (n=45). Visual assessment of the OCA images included criteria for the presence / absence of large blood vessels, of branched networks or of individual vessels, and the presence / absence of a microcapillary network.

2.5. Histological Study

After MM OCT imaging of the intestinal wall the scanned area was marked with histological ink. For histological evaluation, samples were taken after resection of the entire part of the intestine that was being removed according to the plan of surgery. The specimen was fixed in 10% formalin for 48 hours and the histological sections were prepared through the marked areas, so that their planes corresponded to the depth-wise CP OCT images. Haematoxylin and eosin (H&E) staining was used. The histopathologist blinded to the intestinal condition evaluated the histological samples for the presence of edema in the serous and muscle layers and inflammation. He also assessed the state of the blood vessels, following which he classified the samples as either 'normal' 'with a predominance of ischemic tissue damage' (necrosis of individual villi was allowed) or 'widespread tissue necrosis'. Digital photographs were obtained in transmitted light with a Leica DM2500 DFC (Leica Microsystems, Germany) microscope, equipped with a digital camera. The results of the histopathology were compared with the corresponding CP OCT and OCA-based findings.

2.6. Statistical analysis

For statistical data processing the program IBM SPSS Statistics software, V20. (IBM Corporation, Somers, NY, USA) was used. The results are expressed as the Me [Q1; Q3] where Me is the median of the analyzed parameter and [Q1; Q3] are the 25th and 75th percentile values, respectively. To compare the parameters a Kruskal-Wallis analysis of variance (Mann-Whitney U-test with corrected Bonferroni test) was used, where we used: n — the volume of the analyzed subgroup, and p — the magnitude of the statistical significance of the differences. The critical value of the significance level was taken as equal to 5% ($p \leq 0.05$).

3. Results

3.1. MM OCT Study of the Normal Pig Intestine

Porcine small intestine was visualized in vivo with the MM OCT system to establish the methodology. Furthermore, it presented a representation of the intestinal wall microstructure and microcirculation features from the direction of the serous membrane, which is essential for comparison with the subsequent human studies.

Several types of artefacts may be present in OCT [63] and OCA images [64]. In the overwhelming majority of cases, images contain 1 or 2 wide horizontal stripes (Figure 2f, black asterisks) — a consequence of the subject's breathing movements or series of thin, often spaced horizontal lines — the result of heartbeat (pulse waves) [61]. They are most noticeable in the OCA images. The bowel movements itself is best seen in the structural en-face images as a shift of the structures to the left and right with the formation of wavy patterns in the picture.

In the process of recording the MM OCT data, it was found that to minimize motion artefacts in the images, immobility of the tissue relative to the probe surface is required. At the same time, to preserve the true picture of microcirculation, it is important to prevent tissue compression. The probe approaching the intestine should be under the OCT control until a full contact with the entire surface is achieved. After that, the probe must be rigidly fixed, for example with a special holder (we used the holder from KARL STORZ SE & Co. KG, Germany). If the study is carried out without a holder, it is optimal to position the probe and the intestine in a horizontal plane, with a temporary removal of the examined intestinal loop from the laparotomic wound. However, despite all efforts it was almost impossible to completely eliminate all movements and get a real-time image completely free of any artefacts.

The analisys of the porcine structural OCT images in co- and cross- polarization channels (Fig 2c,d,e) based on their comparison with the results of the histological evaluation (Figure 2f) revealed that the depth of visualization of the intestinal wall depends on the muscularis propria and submucosal thickness, but in general, all the layers are potentially clearly visible, including the lamina propria of the mucosa adjacent to the musclaris

mucosa. The structure of the villi themselves are indistinguishable on the structural CP OCT images due to the strong attenuation of the OCT signal at a depth of about 1.3 mm.
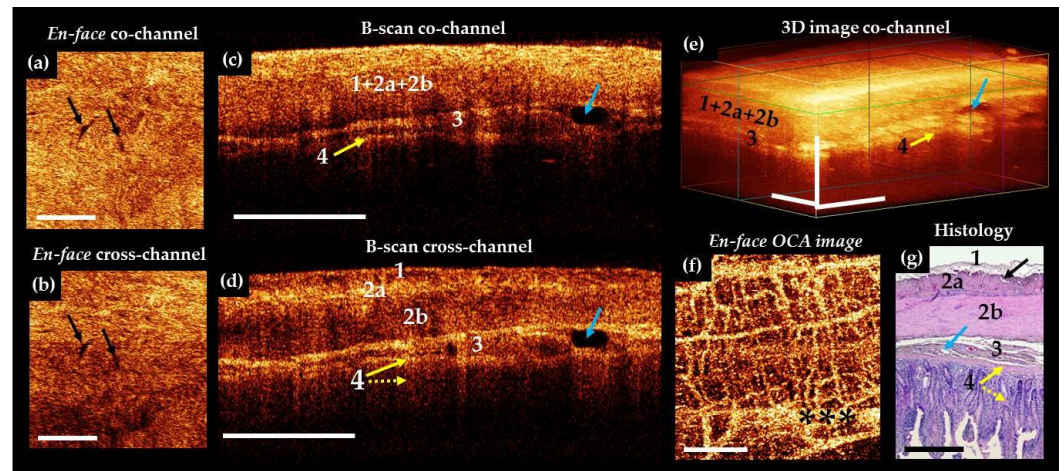
Figure 2. Representative trans-serosal MM OCT images (a-f) and corresponding histology (g) of normal small intestine of a pig. In the B-scans cross-channel (**d**) all 4 layers — serous membrane (1), muscularis externa (longitudinal muscular layer 2a and circular muscular layer 2b), submucosa (3) with blood and lymphatic vessels (blue arrows) and mucosa (4) (in particular, muscularis mucosa (yellow solid arrow) and adjacent to it the lamina propria (yellow dotted arrow)) are more clearly resolved, while in the co-channel not all anatomical layers are optically separated (**c**). (**a, b**) En-face OCT images at the level of the longitudinal muscular layer (green horizontal line in (e)). Intermuscular spaces look like slits and there are few of them (black arrows). In the OCA image (**f**), the network of blood vessels is dense and branched. Large and small blood vessels are visualized; the background of the image is light due to a dense network of a functioning capillary network. (**g**) Histological specimens stained with H&E. Asterisks in (**f**) indicate artefact of motion. Scale bars in CP OCT and OCA images 1 mm, in histology 0.5 mm.

In the B-scans co-polarization channels, as a rule, the serous and muscularis propria are characterized by a high degree of scattering, the intensity of which decreases with depth (Figure 2c, numbers 1,2a,2b). Vertical heterogeneity is created by shadows from the blood vessels of the serous and muscle layers. The vessels themselves are almost indistinguishable on the structural images due to insufficient contrast with the surrounding tissues. The submucosal layer is perfectly visible due to the presence of connective tissue (Figure 2g, number 3) and musclaris mucosa (Figure 2g, number 4, yellow arrow), being visualized as two horizontal stripes (Figure 2c,d, numbers 3 and 4, yellow arrow). Large and small blood and lymphatic (Figure 2c,d, blue arrows) vessels are located in submucosa. It has been established that the cross-polarization image (Figure 2e) provides more information about the layers of the intestinal wall, allowing separate detection of the serosa (Figure 2e, number 1) and the two muscular layers. Note that, the mutually perpendicular arrangement of the muscle layers and the dense parallel packing of the muscle bundles within them leads to polarization effects, as a result of which the outer muscle layer looks brighter than the inner one (Figure 2e, numbers 2 and 3). Similarly, the submucosa (Figure 2e, number 4) is clearly evident due to the sensitivity of polarization to the properties of the collagen fibers forming the connective tissue of this layer. In the en-face OCT images at the level of the outer muscle layer, single slit-like spaces are noticeable (Figure 2a,d, white arrows) which correspond to intermuscular spaces (Figure 2f, black arrow).

In the OCA images of the porcine intestine a dense, branched network of blood vessels can be observed (Figure 2 f). The contours of the large and medium-sized blood vessels are clearly traced, and numerous functioning capillaries create a bright background throughout the image. By varying the depth of visualization of the vasculature and comparing it with the level at which it is visible in the conjugated en-face images, it is possible to analyze the microcirculation in the different layers of the intestinal wall.

After the successful conclusion of the porcine intenstine study, we are now prepared for MM OCT data acquisition from the human intestine in the operating room. An algorithm of actions (methodology) as described above was developed for the upcoming study of the human intestine.

3.2. CP OCT Study of Normal and Ischemic Human Intestine

In vivo MM OCT study of small intestine, performed by trans-serous access, allowed non-invasive visualization of the intestinal wall in all patients to a depth of 1500 to 1800 µm and verification of its layer-by-layer structure. The optical equivalents of the layers of the intestinal wall and the intramural blood vessels were determined by comparing the CP OCT and OCA images with the histological sections precisely made in the same area (Figure 3-6).

Representative CP OCT images of normal human ileum (patients of control group) are shown in Figure 3.
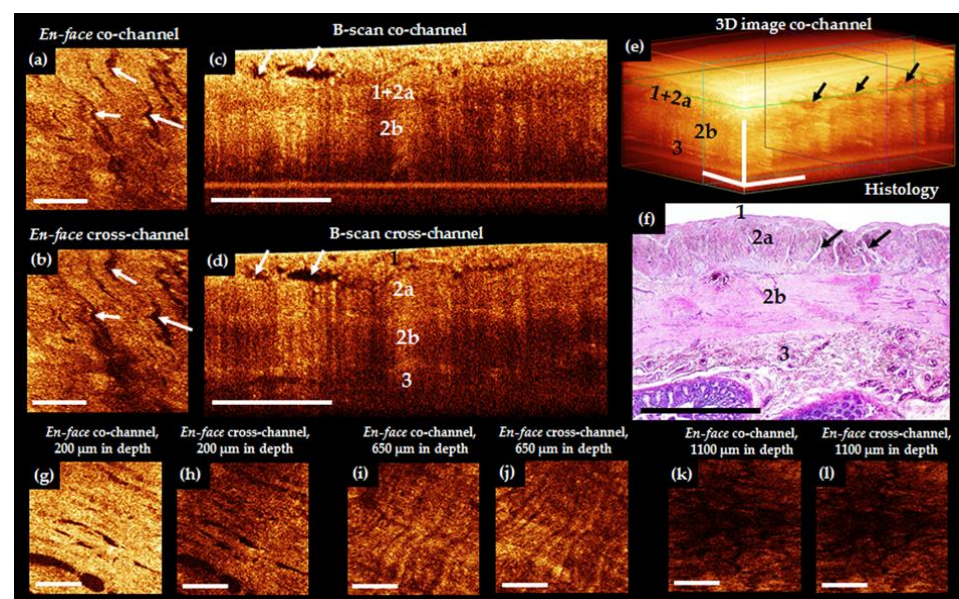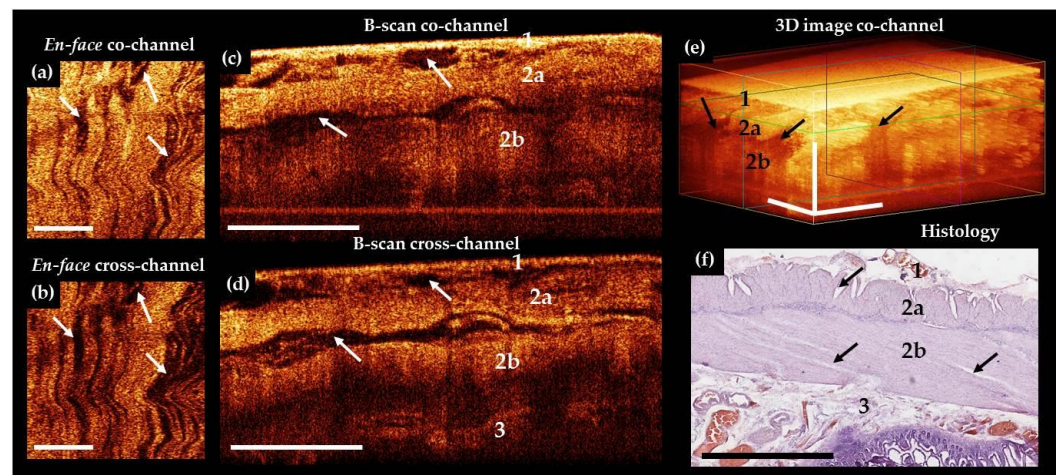

Figure 3. Representative trans-serosal CP OCT images of normal human ileum. In the B-scan cross-channel (**d**) the serous membrane (1), muscularis externa (longitudinal muscular layer 2a and circular muscular layer 2b) and the boundary with submucosa (3) are more clearly resolved, while in the co-channel not all anatomical layers are optically separated (**c, e**). (**a, b**) En-face OCT images at the level of the longitudinal muscular layer (green horizontal line in (**e**)). Intermuscular spaces (**f**, black arrows) look like slits in CP OCT images (**a-d**, white arrows; **e**, black arrows) and they located within the outer muscular layer. (**f**) Corresponding histological image, H&E staining. In some cases, a clear change in the direction of muscle bundles in different layers (**g,h** and **i,j**) and a characteristic pattern of the lamina propria (**k, l**) immediately under the muscularis mucosa can be observed. Scale bars 1 mm.

The results of comparison of OCT B-scans with histological samples revealed that in most cases the intestinal wall visualized in depth to the submucosa. The serous membrane 40–100 µm thick — the first highly scattered layer — practically merges with the underlying muscle layer but is marginally better distinguishable in the cross-channel (Figure 3d, number 1). A distinctive feature of the outer muscle layer (Figure 3c,d,e, number 2a) is its heterogeneity due to the presence of numerous slit-like spaces, which are clearly visible in the en-face images (Figure 3a,b, white arrows). They indicate the location and orientation of the muscle bundles (Figure 3f, black arrows). This layer is up to 400 µm thick. In the co- and cross- channel B-scans, the intermuscular spaces are contrastingly visualized as negative. Note that, the separately located inclusions with a predominantly horizontal orientation (Figure 3c,d, arrows) is due to tissue compression by the probe, whereas, on the corresponding histological specimen, these slit spaces are located at different angles to the surface (Figure 3f, black arrows). The inner (circular) layer of muscle

(Figure 3c,d,e, number 2b) is localized at depth 450–1100 µm, with the zone of transition of the outer muscle layer to the inner one being better defined in the B-scans cross-channel (Figure 3d). This is due to a local increase in the OCT signal intensity and the change of direction of the muscle fibers. The change of direction of the muscle fibers between the different muscle layers (see Figure 3g,h and i,j) can be used when searching for blood vessels, or looking for a layer transition. In some cases submucosa and very rarely part of the mucous membrane (muscularis mucosa and the adjacent to it lamina propria, Figure 3k,l) were visualized. It is possible to visualize in cases of naturally reduced thickness of the muscle and submucosal layers. For example, when the intestinal wall is stretched by a gas bubble located in the lumen of an organ.

Of 18 CP OCT images of normal human small intestine, the serous membrane and muscularis externa were visualized in 18 (100%) of cases, while the submucosa was visible in 12 (66.7%) of 18 of cases, and the mucosa in 2 (11.1%) of 18.

Typical CP OCT images of ischemic, but viable, small intestine of the patients in AMI group are demonstrated in Figure 4.
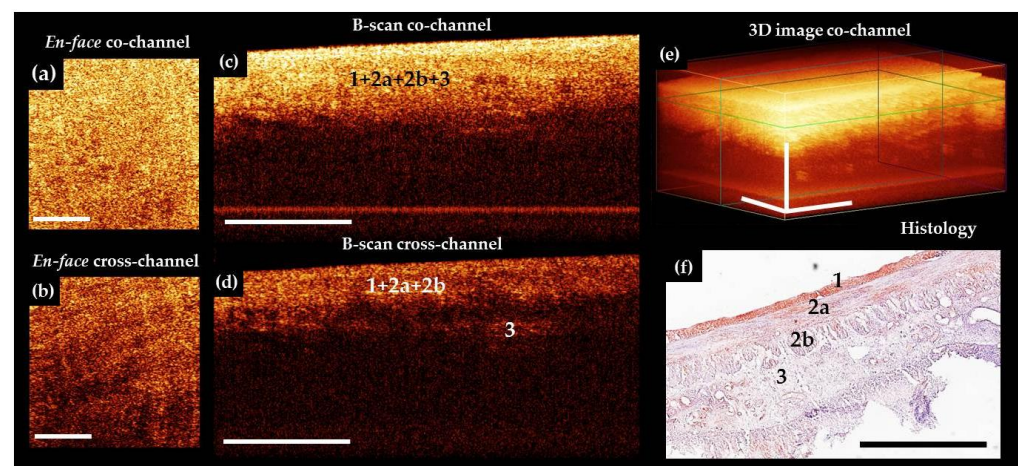

Figure 4. Representative trans-serosal CP OCT images of ischemic ileum without necrosis. (**a, d**) In the B-scans co- (**c**) and cross- (**d**) channels and in 3D OCT image (**e**) the general architecture of the serous membrane (1) and muscularis externa (outer longitudinal - 2a and inner circular - 2b layer of smooth muscle) are clearly resolved with the extensive accumulation of intermuscular fluid (white and black arrows) within each layer. The boundary between the circular muscular layer (2b) and the submucosa (3) is more clearly visible in the B-scan cross-image (**d**). (**a, b**) En-face OCT images at the level of the longitudinal muscular layer (green horizontal line in (**e**)), intermuscular spaces (white arrows) are longer and wider than in norm (Figure 3a,b). (**f**) Corresponding histological image, H&E staining. Black arrows indicate intermuscular edema. Scale bars 1 mm.

Bowel wall thickening was a common finding in the OCT images. Despite external signs of tissue nonviability, in the CP OCT images the general architecture of the outer two layers (serousa and muscularis externa) was preserved, but a large number of well-contoured negative cavities (intermuscular edema) were present in images within all the imaged layers (Figure 4a—d, arrows). Again, in the cross-channel (Figure 4e) the boundary between the circular muscle layer (number 2b) and the submucosa (number 3) is more clearly visible. According to histological analysis, in the adjacent segments of the intestine where the blood supply was partially preserved no transmural necrosis was found (Figure 4f). The manifestations of ischemia in samples of damaged but viable intestine were detected with different frequencies: pronounced edema of the serous and muscle layers in 14 out of 18 cases, and moderate edema in the other 4 cases; thickening, shortening of villi and desquamation of enterocytes 7 out of 18 cases. Necrosis of the submucosa and the muscle layer was not observed. Infiltration of the tissue of the mucous membrane with neutrophils and lymphocytes was also a manifestation of ischemia. It was noted in 14 intestinal samples out of 18. The spread of cellular infiltration into the submucosa and into the muscle layer was noted in 7 cases.

Of 18 CP OCT images of the ischemic small intestine, serous membrane and muscularis externa were visualized in 18 (100%) cases, while submucosa was visible only in 6 (33.3%) cases due to the overall bowel wall thickening.

In a subgroup of AMI patients with histologically confirmed necrosis of most of the intestinal wall, the CP OCT images (Figure 5a-e) appeared structureless and in most cases it was not possible to establish any different layers within the intestinal wall. However, in 4 out of 9 cases the serosa was distinguishable in B-scans co-channel owing to abnormally high scattering of the serous membrane after its impregnation with blood. In 2 (22.2%) out of 9 cases, boundaries between the inner muscle layer and the submucosa were detectable due to a sharp decrease in the signal in the inner muscle layer under cross-channel (Figure 5d, number 3).

Figure 5. Representative trans-serosal CP OCT images of ileum with transmural ischemic necrosis. In the B-scans co- (**c**) and cross- (**d**) channels and in 3D OCT image (**e**) the depth of tissue visualization is decreased significantly and individual layers of the serous membrane (1), outer longitudinal muscular layer (2a) and inner circular muscular layer (2b) are not distinguishable due to the developed necrosis in all layers of the intestinal wall (**f**). In the B-scans cross-channel (d) in the lower part of the inner muscle layer, the signal is noticeably reduced and the transition from this layer to underlying tissue of the submucosa (3) can be detected. (**a, b**) En-face OCT images at the level of the longitudinal muscle layer (green horizontal line in (**e**)), demarcated from the surrounding tissue fluid accumulation is not observed. (**f**) Corresponding histological image, H&E staining. Scale bars 1 mm.

Histological analysis of the intestine with macroscopic signs of transmural necrosis revealed that the thickness of the serous membrane and the two muscle layers was greatly reduced (Figure 5f). All the layers were damaged. Subtotal destruction of villi with desquamation of the enterocytes (in 9 out of 9 cases) was identified in mucosa. Infiltration of preserved fragments of the mucosa and the submucosal layer with neutrophils and eosinophils were observed in 9 out of 9 cases. Furthermore, we observed vascular thrombosis and subtotal vasculature in 8 out of 9 cases, hemorrhagic impregnation of areas of the serous and muscularis propria in 6 out of 9 cases, and foci of lysis of smooth muscle tissue in 4 out of 9 cases.

Thus, the structural OCT conducted via the co- and cross-polarization channels found that:

1) The serous membrane and the outer and internal muscle layers could be visualized in the normal intestine. Furthermore, they could be differentiated from the underlying layers in all observations. In particular, visualization of the submucosa and its differentiation from the muscle layer was feasible in 12 out of 18 cases. The former could be differentiated from the mucosa in 2 out of 18 cases.

2) The ischemic bowel differed from the normal one by the accumulation of intermuscular fluid not only under the serous layer, but also between the bundles of both muscular layers. In contrast to the visualization of necrotic tissues, where the wall stratification

was not observed with MM OCT, in these areas the structure of the outer layer was visible confirming their anatomical integrity. The serous membrane and muscle layers are visualized and can be clearly differentiated in all OCT images, although it was possible to differentiate the submucosa only in 6 out of 18 cases.

3) The necrotic wall of the small intestine appeared structureless in co-channel. In cross-channel, the stratification of layers appeared disturbed. Nevertheless, serosa was distinguishable in 4 out of 9 cases, inner muscular layer from the submucosa — in 2 out of 18 cases. No delimited fluid accumulations were observed in the necrotic intestine.

3.3. OCT Study of Intramural Microcirculation in Normal and Ischemic Human Intestine

In order to exclude the influence of hemodynamic and blood composition parameters among the patients on the quality of visualization of blood vessels using the OCA method , we compared these main indicators in the groups under study. The results are presented in Table 2. There were no statistically significant differences in the analyzed parameters between AMI and control groups (in all cases $p>0.5$).

Table 2. Hemodynamic and blood parameters during MM OCT examination, Me [Q1; Q3].

Parameter	AMI Group	Control Group
Hemodynamics		
Heart rate, beats/min	78 [72; 87]	82 [72; 91]
Systolic arterial pressure, mm Hg	118 [110; 127]	128 [118; 135]
Diastolic arterial pressure, mm Hg	62 [55; 77]	67 [60; 72]
Mean arterial pressure, mm Hg	80 [75; 93]	84 [80; 90]
Central venous pressure, mm Hg	6 [3;10]	8 [4;10]
Peripheral oxygen saturation, %	98 [97;99]	98 [96;99]
Body temperature, ^{0}C	36,5 [36,4;36,9]	36,5 [36,2; 36,8]
Blood		
Le, x10^9/L	12,0 [10; 16,5]	9,2 [8,4; 11,1]
Er, x10^{12}/L	4,1 [3,5; 5,2]	4,1 [3,8; 4,7]
Hb, g/L	131 [124; 141]	123 [111; 137]
Protein, g/L	65 [63,3; 73,3]	69,4 [62; 77,5]

OCA examination of the patient's normal intestine and of parts with ischemia but without necrosis showed that, as a rule, the main part of the perfused vessels could be visualized to a depth of 300 μm, which corresponds to the blood vessels of the serosal and longitudinal muscular layers. In the OCA images, superficially located blood vessels had the appearance of linear branched structures, while the perfused microvascular network created a bright background. Branched vessels of different diameters were visualized in the wall of the non-ischemic intestine (control group) (Figure 6a).

(a)   (b)   (c)
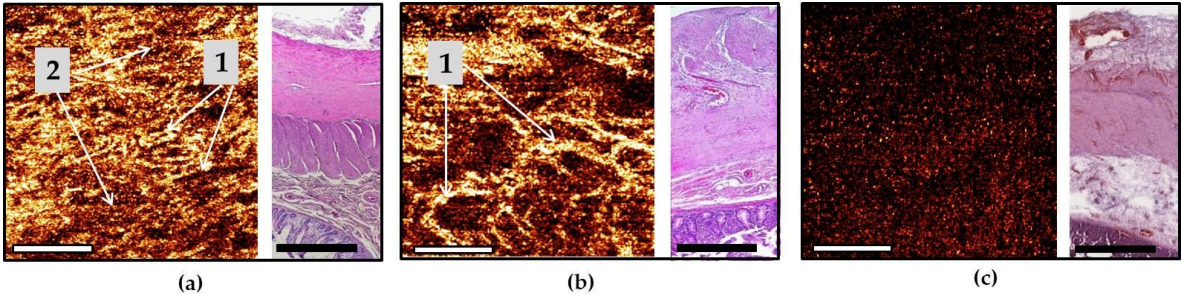
Figure 6. En-face OCA images of the human small intestine in norm and ischemia with the corresponding histology. (**a**) a network of blood vessels of different diameters in the normal intestine wall; (**b**) ischemic bowel without extensive necrosis — noticeable rarefaction of the vasculature and in some areas the background formed by microvessels disappeared; (**c**) ischemic bowel with transmural necrosis. OCA images demonstrate the microvascular network from the tissue surface down to a depth of 500 μm, which corresponds to the blood vessels of the serosal and longitudinal muscular layers. 1 —

intramural blood vessels, 2 — light background from the microvessels. Histological specimens are stained with H&E. Scale bars 1 mm.

The vasculature was visible in all the patients of the control group, despite the fact that motion artefacts (bright thin, and wide horizontal stripes) were inevitably present on the OCA images (Figure 6a). Histological examination confirmed the presence of non-damaged blood vessels in the serous membrane, with large vessels penetrating the peritoneum and spreading into the subserous space, while there were also numerous arterioles and venules penetrating the muscle layers of the intestinal wall. No ischemic injuries were found in this group of patients (Figure 6a).

In patients with AMI, the optical equivalents of the vessels differed significantly in areas with irreversible changes (necrosis) and in viable ischemic tissue. In areas with irreversible ischemic injury and necrosis, blood vessels either could not be visualized at all on the OCA images or only showed as single vessels, while the background of the angiogram was homogeneous and predominantly dark (Figure 6c). In areas with histologically confirmed viable ischemic tissue, the OCA images revealed a few blood vessels of different diameters, but they were fragmentary and did not form a network. The background of the OCA image was predominantly dark due to the loss of capillaries, small arterioles and venules (Figure 6b). The histological picture in this case included ischemic damage to the vascular system in the form of the presence of a plethora of mostly large blood vessels in stasis with sludge in some of the vessels, while almost all the capillaries were in stasis (Figure 6b). Therefore, the capillaries were not visualized on the OCA images.

In accordance with the approaches [65,66] and the experience of our group with experimental studies [15], a full (i.e. effective) intramural microcirculation requires the presence of blood flow in two components of the microvascular network: 1 — in the intramural arteries that anastomose with the vessels of adjacent sections of the intestine; 2 — in the microvascular network of the submucosa. We found that both of these conditions are met in the normal state. In ischemia without necrosis, the intramural arteries could be visualized, but did not form a continuous network; at the level of the submucosal layer, the vessels were distinguishable in (33.3%) 6 out of 18 cases. This fact suggests that in this case, ischemia is of a non-occlusive nature. Measures aimed at enhancing the bloodstream could transition a situation with ischemia towards an increase in the number of perfused vessels, starting the processes of restoring the structural integrity of the damaged sections of the intestine. In cases of ischemia with transmural necrosis, no perfused large or small blood vessels could be observed, indicating a completely impaired blood flow in these areas. Visually, they could also be recognized as non-viable and were therefore subject to mandatory resection.

A comprehensive analysis of MM OCT of the small intestine has thus revealed significant differences in the qualitative characteristics of its microstructure and microcirculation in patients with normal intestines and those with AMI. Table 3 summarizes this data.

Table 3. Characteristics of MM OCT features of the small intestine in studied groups of patients. n- number of regions of interest (ROI).

Group of ROI	Structural OCT features						Angiographic OCT features		
	Detectable layers of small intestine, n-Abs. (%)					Inter-muscular spaces	Subserosal blood vessels	Micro-vascular network	OCA description
	Serosa	Outer Muscular Layer	Inner Muscular Layer	Sub mucosa	Mucosa				
Control Group (n=18)	18 (100)	18 (100)	18 (100)	12 (66.7)	2 (11.1)	narrow slit-like spaces between the muscle bundles localized of only within the outer muscular layer	yes	yes	Multiple branched blood vessels anastomosed with each other, the background is light

AMI Group	Ischemia **(n=18)**	18 (100)	18 (100)	18 (100)	6* (33.3)	-	wide numerous spaces localized between the muscle bundles of the both muscular layers, as well as at the borders of the serous and outer muscular layers and of the outer and inner muscular layers	yes	partly	sparse vasculature or single, predominantly non-anastomosed blood vessels with each other, the background is mostly dark
	Necrosis **(n=9)**	4 (44.4)	-		2* (22.2)	-	no	no	no	Scraps of single blood vessels or their complete absence, the background is dark

* - only the boundary between the inner muscular layer and submucosa was distinguished.

4. Discussion

The technologies used for accurate topical diagnosis of ischemia in the organs of the digestive tract are focused on identifying qualitative and quantitative parameters of blood flow during surgery and predicting the risk of ischemic necrosis. For emergency surgery in cases of AMI, the possibility of simultaneous visualization of the perfused microvessels along with assessing the state of the layers of the intestinal wall at each point of interest is particularly valuable for the surgeon. Multidetector computed tomography with intravenous contrast is the main method of screening diagnostics and preoperative examination of a patient with suspected AMI [8], but it is not suitable for intraoperative use. The method is able to verify the occlusion of arteries (as a rule, extramural) with a diameter of more than 1000 μm [67], but are not suitable for accurate mapping or diagnosis of blood flow in intramural vessels. During surgery, LDF, FI, SDF, IDF, LSCI, HIS and OCA can be helpful to determine the intestine viability and clarify the exact border of bowel resection [43–45,68]. LDF, FI, SDF, IDF, LSCI, HIS techniques obtain information about perfusion/blood flow and only OCA assesses bowel microvessels and microstructure simultaneously [49].

The suitability of each method in the spectrum of diagnostic technologies for intestinal ischemia is determined by its resolution, visualization depth, dimensions of the field of view and the ability to quantify data [43–45,68]:

1) The resolution should be sufficient to detect microvessels and tissue structural features. Image resolution of IDF (3.3 μm), LSCI (10 μm) and OCA (5-15 μm) is greater than in SDF (30-50 μm) and FI (450 μm), which is enough for capillary visualization. Conventional LDF offers no image, only measurements in digital format.

2) The imaging depth should be sufficient to reveal structural or blood flow changes not only in the superficial layers (serous membrane and muscularis externa), but also in a deeply localized tissue (the submucosa and mucous layers), from where necrosis begins. Maximal imaging depth of IDF, SDF and LDF is about the same and is 0.5 mm, which is rather small for a complete picture of gut microcirculation. Other methods allow seeing deep into the tissue up to 1 mm with LSCI, 1-1.5mm with FI, 1.5-2 mm with OCA and 1-6 mm with HIS, therefore they are better suited for diagnostic purposes.

3) Considering that the gut has a large surface area, the size of the field of view of the optical method is also important when it is inspected for the boundaries of the viable tissues. From this position, the FI method has an undeniable advantage. It allows assessing the entire length of the intestine at once. Field of view of LSCI and HIS is measured from a few square centimeters to several tens of square centimeters. It is also sufficient for assessing large bowel surfaces. OCT-A visualizes from 9-10 mm² to 100 mm², while IDF and SFD have the smallest field of view (1-2 mm²);

4) Quantification of data objectifies them, allowing for finding the exact criteria for separating two states. The IDF and SFD methods have an advantage in quantification of vascular networks: at least 4 microcirculatory parameters can be calculated (total and perfused vessel density, the proportion of perfused vessels, the microvascular flow index).

Other methods (OCT-A, LDF, LSCI and HIS) also have a quantitative expression of blood perfusion data using already developed and tested methods, while the first attempts at quantifying the fluorescence signal were made for FI [29].

In conclusion, a comparison of the main characteristics of optical methods showed that each has certain advantages and limitations. The strengths of a specific technology are used to address a specific clinical problem. In contrast to the other methods considered, OCA is the best technology for the purposes of bowel diagnostics with AMI due to sufficient resolution (15 μm) and scanning depth (˜1.8 mm). Based on the received data, MM OCT provides three-dimensional data that are researcher-friendly without any additional post-processing. It allows visual assessment of both the structure and the microcirculation of the intestinal wall. Data quantification is also possible. The ability to obtain the combination of structural and angiographic data is the key characteristic distinguishing MM OCT from other similar diagnostic technologies.

Using MM OCT, we managed to achieve a high quality of visualization of the complex of serous and muscle layers and the vascular network localized within them. It should be emphasized, that useful and clinically significant results of the study of muscle fibers have previously been demonstrated by high-frequency ultrasound scanning of the rectal muscular layer [69]. However, CP OCT technology is an improvement as it offers imaging of individual muscle bundles and intermuscular spaces with higher resolution and contrast. The possibilities of their use for trans-serous intestinal studies have not yet been investigated. Other currently used optical methods for microcirculation imaging in the gastrointestinal tract (for example, SDF, LDF, NIR resonance spectrometry), as a rule, allow assessing changes in perfusion, but do not directly verify necrotic tissue [32]. Due to the irregular sensitivity of the layers of the intestinal wall to ischemia, blood vessels can remain in one layer when necrosis of another has already developed. Therefore, the ability of OCT to blood flow detection simultaneously with a tissue microstructure (determination of its viability or necrosis) is an important diagnostic advantage.

Along with the quality of the data obtained, the required duration of the investigative procedure is an important factor from a clinical point of view. In our pilot study [70] we have established that it takes only 8 to 12 minutes to obtain the 5–8 MM OCT images that are required to verify the depth of ischemic injury. That is, the time required for MM OCT is only 6–10% of the total duration of the typical AMI operation, thus significantly minimizing the period of anesthesia requirement and "open abdominal" state.

Our experience of experimental and clinical research has shown that the data obtained on the AMI model in laboratory animals could only partially be extrapolated to clinical diagnosis in patients. OCA of the small intestine of patients has shown both similarities and differences from the data obtained in experiment on laboratory animals (rats, miniature pigs) [49,59]. Apparently, the differences in the OCA picture of the small intestine (both in the norm and in ischemia) between laboratory animals and humans are due to the anatomical and physiological parameters of the vascular system of the small intestine, namely, the thickness and optical density of the serous membrane, the depth of the location of large vessels, their diameter and the blood flow rate. In an experiment on animals [49], we have previously identified diagnostically significant criteria for the preservation of intramural intestinal blood flow: 1 — the presence of large "treelike", often paired, vessels with a diameter of 50–200 μm; 2 — a uniformly light background to the OCA image, the presence of which depends on the functioning of the arterioles, venules and capillaries of the submucosa and mucosa. In the OCA images of an ischemic but viable human intestine, these criteria were met in no more than 70% of observations. In the present study, out of a total of 60 OCA images obtained from 18 patients, 15 (25%) of them contained significant artefacts: light stripes caused by intestinal peristaltic waves; the patient's breathing movements; or pulse vibrations of the abdominal aorta. It is known that in other bioimaging methods used for angiography of the intramural bed of the intestine, peristaltic bowel movements are also the cause of rejection of 10–15% of images [21].

Group of Ton G. van Leeuwen (University of Amsterdam, The Netherlands) used a commercially available OCT system for detection of blood flow of gastric tissue after

esophagectomy in order to reduce post-operative complications due to impaired perfusion [58]. The results showed the feasibility of intra-operative OCT-based imaging of gastric tissue and detection of flow in blood vessels in patients with esophageal cancer. 3D OCT data were obtained but microcirculatory was demonstrated as blood vessel locations in structural B-scans. The idea was to distinguish areas with flow from static tissue, which became possible after speckle contrast (the ratio of speckle variance over the mean) calculation from OCT M-mode scans. The percentage of pixels distinguished as flow was quantified as an objective parameter that can potentially be used to differentiate normal from decreased perfusion areas. In this study the focus was placed on speckle contrast to show blood flow, while the structural images themselves were not analyzed. The authors faced with the problem of motion artefacts induced by the surgeon's hand as well as the patient's heartbeat and breathing, therefore they failed to visualize blood vessel in the 3D OCT. It was also emphasized that quality of the images was suboptimal as stabilization of the OCT probe was very difficult.

Building on the impressive result of [58], we were the first to demonstrate en-face 2D images of blood vessels network in normal and ischemic human intestine, obtained *in vivo* during extempore surgery [70]. OCA images were shown without any post-processing like those presented in the current work. This has been done in order to show the native images and artefact problems that are present when obtaining OCA images in a real clinical setting. Of course, post-processing can significantly improve the OCA image quality for the visualization of the microcirculatory network, but as practice shows, it can also cause the loss of some important information about the vessels in doing so. Thus, together with the artefacts, vessels of a certain diameter may also be removed from the image, thereby impairing the reliability of the information. In this work, the goal was not to provide accurate quantification of the vascular networks, so presenting the material without post-processing is acceptable. In such cases, the vascular networks can be traced as brighter linear structures with clear outlines against a background of various kinds of noise.

Only one study was found, which presents the results of OCT imaging of the gastric wall structure from the side of the serous membrane [58]. The emphasis was placed on the blood vessels detection in OCT images while OCT features in norm and ischemia were not described in detail. Prior to the current research, OCT visualization of the intestinal wall was not performed trans-serosally. We believe the reason is, first of all, insufficient scanning depth for observing the mucous membrane, including the villi, from where irreversible changes begin in ischemia. When studying ischemic injury, the attention of researchers is usually focused on the processes occurring in the mucous membrane. In our study, we showed that structural imaging of the outer layers up to the submucosa, combined with the microvascular network visualization, is sufficient to understand the depth of tissue damage.

The advantage of the used MM OCT setup is the presence of a cross-polarization channel. It provides a more contrasting visualization of the intestinal layers: the OCT signal is enhanced from polarization-sensitive structures (collagen and muscle fibers which is well organized in space) while is weakened from structures that do not have such properties, only backward scattering. Thus, multimodality OCT imaging with polarization sensitivity is a promising instrument for intraoperative assessment of bowel viability.

There are some limitations of the study, which needs mentioning. Firstly, only a relatively small number of patients (18 persons) were enrolled; therefore, the result obtained at this stage is, essentially, a feasibility study to assess the information content and safety of MM OCT in the emergency diagnosis of human small intestine pathology. The final formulation of MM OCT diagnostic criteria for bowel pathology requires further accumulation of clinical data. Secondly, the MM OCT results in the control group cannot be fully accepted as a standard for intact human small intestine. Structural and functional changes in the "histologically intact" intestinal segments in patients with colorectal cancer are caused by epigenetic, microbiological and biochemical factors; thus their long-term influence could have caused changes in the microstructure of the tissues and, accordingly, in

the OCT picture of the ileal wall. However, based on the data presented, it can be argued that the presence of characteristic microstructural changes in the intestinal wall caused by acute ischemic injury (AMI group) is clearly contrasted with the intestine not damaged by AMI (control group).Therefore, at this stage of research it would be premature to recommend the routine use of MM OCT as a self-contained method for assessing the viability of sections of ischemic bowel. However, after elimination of limitations described above, the method could become one of the main techniques for the clinical diagnosis of the extent of intestinal tissue damage in AMI.

5. Conclusions

MM OCT allows simultaneous assessment of structure and microcirculation with high resolution, which is crucial for clinicians in defining the boundaries of bowel resection in AMI. Intraoperative MM OCT performed by trans-serous access is a potential diagnostic tool for objective assessment of the condition of intestinal wall layers along with the vessels localized within them. The MM OCT images of non-ischemic, ischemic, viable and necrotic small intestine differ significantly in the volume of extravasal fluid accumulation, the structure of muscle bundles in the longitudinal muscle layer, and the type and density of the vasculature.

The MM OCT diagnostic procedure optimally meets the requirements of emergency surgery as it requires relatively less time to examine the microstructure and microcirculation of the intestine along its entire length from the direction of the serous membrane without resorting to transluminal interventions and contrasts. Optionally, the MM OCT data can include objective quantitative parameters. Despite the advantages, MM OCT method of data acquisition requires significant improvement in order to reduce the number of motion artefacts. In actual clinical conditions it may not be as effective as in a laboratory condition. Application on animals in a controlled laboratory environment allows for maximal stabilization of the moving system parts and the studied organ which is near impossible to replicate under actual clinical condition.

References

1. Patel: A.; Kaleya, R.N.; Sammartano, R.J. Pathophysiology of mesenteric ischemia. *Surg. Clin. North Am.* **1992**, *72*, 31-41.
2. Bala, M,; Kashuk, J.; Moore, E.E.; Kluger, Y.; Biffl, W.; Gomes, C.A.; Ben-Ishay, O.; Rubinstein, C.; Balogh, Z.J.; Civil, I.; Coccolini, F.; Leppaniemi, A.; Peitzman, A.; Ansaloni, L.; Sugrue, M.; Sartelli, M.; Di Saverio, S.; Fraga, G.P.; Catena, F. Acute mesenteric ischemia: guidelines of the World Society of Emergency Surgery. *World J. Emerg. Surg.* **2017,** *12*, 38:1-11.
3. Rodriguez-Nakamura, R.M.; Gonzalez-Calatayud, M.; Martinez, A.R. Acute mesenteric thrombosis in two patients with COVID-19. Two cases report and literature review. *Int. J. Surg. Case Rep.* **2020**, *76*, 409-414.

4.   Fan, B.E.; Chang, C.C.R.; Teo, C.H.Y.; Yap, E.S. COVID-19 Coagulopathy with Superior Mesenteric Vein Thrombosis Complicated by an Ischaemic Bowel. *Hamostaseologie* **2020**, *40*, 592-593.

5.   Azouz, E.; Yang. S.; Monnier-Cholley, L.; Arrivé, L. Systemic arterial thrombosis and acute mesenteric ischemia in a patient with COVID-19. *Intensive Care Med.* **2020**, *46*, 1464-1465.

6.   Khesrani, L.S; Chana, K.; Sadar, F.Z.; Dahdouh, A.; Ladjadj, Y.; Bouguermouh, D. Intestinal ischemia secondary to Covid-19. *J. Pediatr. Surg. Case Rep.* **2020**, *61*, 101604:1-5.

7.   Acosta, S. Mesenteric ischemia. *Curr. Opin. Crit. Care* **2015**, *21*, 171–178.

8.   Mastoraki, A.; Mastoraki ,S.; Tziava, E.; Touloumi, S.; Krinos, N.; Danias, N.; Lazaris, A,; Arkadopoulos, N. Mesenteric ischemia: pathogenesis and challenging diagnostic and therapeutic modalities. *World J. Gastrointest. Pathophysiol.* **2016**, *7*, 125–130.

9.   Bulkley, G.B.; Zuidema, G.D.; Hamilton, S.R.; O'Mara, C.S.; Klacsmann, P.G.; Horn, S.D. Intraoperative determination of small intestinal viability following ischemic injury: a prospective, controlled trial of two adjuvant methods (Doppler and fluorescein) compared with standard clinical judgment. *Ann. Surg.* **1981**, *193*, 628-37.

10. Herbert, G.S.; Steele, S.R. Acute and chronic mesenteric ischemia. *Surg. Clin. North Am.* **2007**, *87*, 1115-34, ix.

11. Caluwaerts, M.; Castanares-Zapatero, D.; Laterre, P.-F.; Hantson, P. Prognostic factors of acute mesenteric ischemia in ICU patients. *BMC Gastroenterol.* **2019**, *19*, 80:1-10.

12. Yang, S.; Zhao, Y.; Chen, J.; Ni, Q.; Guo,; Huang, X.; Xue, G.; Zhang, L. Clinical Features and Outcomes of Patients With Acute Mesenteric Ischemia and Concomitant Colon Ischemia: A Retrospective Cohort Study. *J. Surg. Res.* **2019**, *233*, 231-239.

13. Johansson, K.; Ahn, H.; Lindhagen, J. Assessment of small-bowel ischemia by laser Doppler flowmetry. Some case reports. *Scand. J. Gastroenterol.* **1986**, *21*, 1147-1152.

14. Avino, A.J.; Oldenburg, W.A.; Gloviczki, P.; Miller, V.M.; Burgart, L.J.; Atkinson, E.J. Inferior mesenteric venous sampling to detect colonic ischemia: a comparison with laser Doppler flowmetry and photoplethysmography. *J Vasc Surg.* **1995**, *22*, 271-277.

15. Redaelli, C.A.; Schilling, M.K.; Buchler, M.W. Intraoperative laser Doppler flowmetry: a predictor of ischemic injury in acute mesenteric infarction. *Dig. Surg.* **1998**, *15*, 55-59.

16. Kaser, S.A.; Glauser, P.M.; Maurer, C.A. Venous small bowel infarction: intraoperative laser Doppler flowmetry discriminates critical blood supply and spares bowel length. *Case Rep. Med.* **2012**, *2012*, 195926:1-3.

17. Gordeeva, A.E.; Sharapov, M.G.; Tikhonova, I.V.; Chemeris, N.K.; Fesenko, E.E.; Novoselov, V.I.; Temnov, A.A. Vascular Pathology of Ischemia/Reperfusion Injury of Rat Small Intestine. *CTO.* **2017**, *203*, 353-364.

18. Horstmann, R.; Palmes, D.; Rupp, D.; Hohlbach, G.; Spiegel, H.U. Laparoscopic fluorometry: a new minimally invasive tool for investigation of the intestinal microcirculation. *J. Invest. Surg.* **2002**, *15*, 343-350.

19. Liot, E.; Assalino, M.; Buchs, N.C., Schiltz, B.; Douissard, J.; Morel, P.; Ris, F. Does near-infrared (NIR) fluorescence angiography modify operative strategy during emergency procedures? *Surg Endosc.* **2018**, 32, 4351-4356.

20. Karampinis, I.; Keese, M.; Jakob, J.; Stasiunaitis, V.; Gerken, A.; Attenberger, U.; Post, S.; Kienle, P.; Nowak, K. Indocyanine Green Tissue Angiography Can Reduce Extended Bowel Resections in Acute Mesenteric Ischemia. *J. Gastrointest. Surg.* **2018**, *22*, 2117–2124.

21. Khripun, A.I.; Priamikov, A.D.; Shurygin, S.N.; Mironkov, A.B.; Petrenko, N.V.; Grigor'eva, S.G.; Latonov, V.V.; Abashin, M.V.; Izvekov, A.A. [The possibilities of laser Doppler flowmetry for the estimation of the intestine resection volume by the acute mesenteric ischemia]. *Khirurgiia (Mosk).* **2012**, *10*, 40-44.

22. Yalcin, D.; Saçak, B.; Yalcin, M.; Yildirim, A.; Karademir, B.; Ercan, F.; Celebiler, Ö. Intraluminal fluid infusion in a rat jejunum ischemia/reperfusion model is associated with improved tissue perfusion and less mucosal damage. *J. Plast. Reconstr. Aesthet. Surg.* **2020**, *73*, 590-597.

23. Toropova, Y.G.; Pechnikova, N.A.; Zelinskaya, I.A.; Zhuravsky, S.G.; Kornyushin, O.V.; Gonchar, A.I.; Ivkin, D.Y.; Leonova, Y.V.; Karev, V.E.; Karabak, I.A. Nicotinamide riboside has protective effects in a rat model of mesenteric ischaemia-reperfusion. *Int. J. Exp. Pathol.* **2018**, *99*, 304-311.

24. Berge, S.T.; Safi, N.; Medhus, A.W.; Ånonsen, K,; Sundhagen, J.O,; Hisdal, J.; Kazmi, S.S.H. Gastroscopy assisted laser Doppler flowmetry and visible light spectroscopy in patients with chronic mesenteric ischemia. *Scand. J. Clin. Lab. Invest.* **2019**, *79*, 541-549.

25. Berge, S.T.; Safi, N.; Medhus, A.W.; Sundhagen, J.O.; Hisdal, J,; Kazmi, S.S.H. Perioperative Microcirculatory Changes Detected with Gastroscopy Assisted Laser Doppler Flowmetry and Visible Light Spectroscopy in Patients with Median Arcuate Ligament Syndrome. *Vasc. Health Risk Manag.* **2020**, *16*, 331-341.

26. Su, H.; Wu, H.; Bao, M.; Luo, S.; Wang, X.; Zhao, C.; Liu, Q.; Wang, X.; Zhou, Z.; Zhou, H. Indocyanine green fluorescence imaging to assess bowel perfusion during totally laparoscopic surgery for colon cancer. *BMC Surg.* **2020**, *20*, 102:1-7.

27. Björck, M.; Koelemay, M.; Acosta, S.; Goncalves, B.; Kölbel, T.; Kolkman, J.J.; Lees, T.; Lefevre, J.H.; Menyhei, G.; Oderich, G. Editor's Choice – Management of the Diseases of Mesenteric Arteries and Veins. Clinical Practice Guidelines of the European Society of Vascular Surgery (ESVS). 2017. *Eur. J. Vasc. Endovasc. Surg.* **2017**, *53*, 460-510.

28. Ballard, J.L.; Stone, W.M.; Hallett, J.W.; Pairolero, P.C.; Cherry, K.J. A critical analysis of adjuvant techniques used to assess bowel viability in acute mesenteric ischemia. *Am. Surg.* **1993**, *59*, 309-311.

29. Barberio, M.; Felli, E.; Seyller, E.; Longo, F.; Chand, M.; Gockel, I.; Geny, B.; Swanström, L.; Marescaux, J.; Agnus, V.; Diana, M. Quantitative fluorescence angiography versus hyperspectral imaging to assess bowel ischemia: A comparative study in enhanced reality. *Surgery* **2020**, *168*, 178-184.

30. De Bruin, A.F.; Kornmann, V.N.; van der Sloot, K.; van Vugt, J.L.; Gosselink, M.P.; Smits, A.; Van Ramshorst, B.; Boerma, E.C.; Noordzij, P.G.; Boerma, D.; van Iterson, M. Sidestream dark field imaging of the serosal microcirculation during gastrointestinal surgery. *Colorectal Dis.* **2016**, *18*, O103-O110.

31. De Bruin, A.F.J. ; Tavy, A.L.M. ; van der Sloot, K. ; Smits, A.; Ince, C.; Boerma, E.C.; Noordzij, P.G.; Boerma, D.; van Iterson, M. Can sidestream dark field (SDF) imaging identify subtle microvascular changes of the bowel during colorectal surgery? *Tech. Coloproctol.* **2018**, *22*, 793-800.

32. Jansen, S.M.; de Bruin, D.M.; van Berge Henegouwen, M.I.; Bloemen, P.R,; Strackee, S.D.; Veelo, D.P.; van Leeuwen, T.G.; Gisbertz, S.S. Quantitative change of perfusion in gastric tube reconstruction by sidestream dark field microscopy (SDF) after esophagectomy, a prospective in-vivo cohort study. *Eur. J. Surg. Oncol.* **2020**, *S0748-7983*, 30776-9.

33. Uz, Z.; Kastelein, A.W.; Milstein, D.M.J.; Liu D.; Rassam, F.; Veelo, D.P.; Roovers, J.-P.W.R.; Ince C.; van Gulik, T.M. Intraoperative Incident Dark Field Imaging of the Human Peritoneal Microcirculation. *J. Vasc. Res.* **2018**, *55*, 136-143.

34. Tavy, A.L.M.; de Bruin, A.F.J.; Smits, A.B.; Boerma, E.C.; Ince, C.; Noordzij, P.G.; Boerma, D.; van Iterson, M. Intestinal Mucosal and Serosal Microcirculation at the Planned Anastomosis during Abdominal Surgery. *Eur. Surg. Res.* **2019**, *60*, 248-256.

35. Mehdorn, M.; Köhler, H.; Rabe, S.M.; Niebisch, S.; Lyros, O.; Chalopin, C.; Gockel, I.; Jansen-Winkeln, B. Hyperspectral Imaging (HSI) in Acute Mesenteric Ischemia to Detect Intestinal Perfusion Deficits. *J. Surg. Res.* **2020**, *254*, 7-15.

36. Holmer, A.; Tetschke, F.; Marotz, J.; Malberg, H.; Markgraf, W.; Thiele, C.; Kulcke, A. Oxygenation and perfusion monitoring with a hyperspectral camera system for chemical based tissue analysis of skin and organs. *Physiol. Meas.* **2016**, *37*, 2064-2078.

37. Ambrus, R,; Strandby, R.B,; Svendsen, L.B.; Achiam, M.P.; Steffensen. J.F.; Søndergaard Svendsen, M.B. Laser Speckle Contrast Imaging for Monitoring Changes in Microvascular Blood Flow. *Eur. Surg. Res.* **2016**, *56*, 87-96.

38. Heeman, W.; Dijkstra, K.; Hoff.; C, Koopal, S.; Pierie, J.P.; Bouma, H.; Boerma, E.C. Application of laser speckle contrast imaging in laparoscopic surgery. *Biomed. Opt. Express* **2019**, *10*, 2010-2019.

39. Milstein, D.M.J.; Ince, C.; Gisbertz, S.S.; Boateng, K.B.; Geerts, B.F.; Hollmann, M.W.; van Berge Henegouwen, M.I.; Veelo, D.P. Laser speckle contrast imaging identifies ischemic areas on gastric tube reconstructions following esophagectomy. *Medicine (Baltimore)* **2016**, *95*, e3875:1-8.

40. Ambrus, R.; Achiam, M.P.; Secher, N.H.; Svendsen, M.B.S.; Rünitz, K.; Siemsen, M.; Svendsen, L.B. Evaluation of gastric microcirculation by laser speckle contrast imaging during esophagectomy. *J. Am. Coll. Surg.* **2017**, *225*, 395–402.

41. Kojima, S.; Sakamoto, T.; Nagai, Y.; Matsui, Y.; Nambu, K.; Masamune, K. Laser Speckle Contrast Imaging for Intraoperative Quantitative Assessment of Intestinal Blood Perfusion During Colorectal Surgery: A Prospective Pilot Study. *Surg. Innov.* **2019**, *26*, 293-301.

42. Zheng, C.; Lau, L.W.; Cha, J. Dual-display laparoscopic laser speckle contrast imaging for real-time surgical assistance. *Biomed. Opt. Express* **2018**, *9*, 5962-5981.

43. Urbanavičius, L.; Pattyn, P,; de Putte, D.V.; Venskutonis, D. How to assess intestinal viability during surgery: A review of techniques. *World J. Gastrointest. Surg.* **2011**, *3*, 59-69.

44. Jansen, S.M.; de Bruin, D.M.; van Berge Henegouwen, M.I.; Strackee, S.D.; Veelo, D.P.; van Leeuwen, T.G.; Gisbertz, S.S. Optical techniques for perfusion monitoring of the gastric tube after esophagectomy: a review of technologies and thresholds. *Dis. Esophagus* **2018**, *31*, dox161:1-11.

45. Bryski, M.G.; Frenzel Sulyok, L.G.; L. Kaplan, S. Singhal, Keating, J.J. Techniques for intraoperative evaluation of bowel viability in mesenteric ischemia: A review. The American Journal of Surgery. 2020. 220, 309-315.

46. Kashani, A.H.; Chen, C.L.; Gahm, J.K.; Zheng, F.; Richter, G.M.; Rosenfeld, P.J.; Shi, Y.; Wang, R.K. Optical coherence tomography angiography: A comprehensive review of current methods and clinical applications. *Prog. Retin. Eye Res.* **2017**, *60*, 66-100.

47. Gora, M.J.; Suter, M.J.; Tearney, G.J.; Li, X. Endoscopic optical coherence tomography: technologies and clinical applications [Invited]. *Biomed. Opt. Express* **2017**, *8*, 2405-2444.

48. Tsai, T.H.; Leggett, C.L.; Trindade, A.J.; Sethi, A.; Swager, A.F.; Joshi, V.; Bergman, J.J.; Mashimo, H.; Nishioka, N.S.; Namati, E. Optical coherence tomography in gastroenterology: a review and future outlook. *J. Biomed. Opt.* **2017**, *22*, 1-17.

49. Ryabkov, M.G.; Kiseleva, E.B.; Baleev, M.S.; Bederina, E.L.; Sizov, M.A.; Vorobyov, A.N.; Moiseev, A.A.; Karabut, M.M.; Plekhanova, M.A.; Gladkova, N.D. Trans-serosal multimodal optical coherence tomography for visualization of microstructure and blood circulation of the small intestine wall. *STM* **2020**, *12*, 56-64.

50. Gora, M.G., Tearney, G.J. Enhanced Imaging of the Esophagus: Optical Coherence Tomography. In *Barrett's Esophagus: Emerging Evidence for Improved Clinical Practice*, 1st ed.; Pleskow, D.K., Erim, T., Eds.; Academic Press: London, UK, 2016; pp. 105-122.

51. Zuccaro, G.; Gladkova, N.; Vargo, J.; Feldchtein, F.; Zagaynova, E.; Conwell, D.; Falk, G.; Goldblum, J.; Dumot, J.; Ponsky, J.; Gelikonov, G.; Davros, B.; Donchenko, E.; Richter J. Optical coherence tomography of the esophagus and proximal stomach in health and disease. *Am. J. Gastroenterol.* **2001,** *96*, 2633-2639.

52. Das, A.; Sivak Jr., M.V.; Chak, A.; Wong, R.C.; Westphal, V.; Rollins, A.M.; Willis, J.; Isenberg, G.; Izatt, J.A. High-resolution endoscopic imaging of the GI tract: a comparative study of optical coherence tomography versus high-frequency catheter probe EUS. *Gastrointest. Endosc.* **2001,** *54*, 219-224.

53. Tsai, T.H.; Lee, H.C.; Ahsen, O.O.; Liang, K.; Giacomelli, M.G.; Potsaid, B.M.; Tao, Y.K.; Jayaraman, V.; Figueiredo, M.; Huang, Q.; Cable, A.E.; Fujimoto, J.; Mashimo, H. Ultrahigh speed endoscopic optical coherence tomography for gastroenterology. *Biomed. Opt. Express* **2014,** *5*, 43870-4404.

54. Hatta, W.; Uno, K.; Koike, T.; Yokosawa, S.; Iijima, K.; Imatani, A.; Shimosegawa, T. Optical coherence tomography for the staging of tumor infiltration in superficial esophageal squamous cell carcinoma. *Gastrointest. Endosc.* **2010,** *71*, 899–906.

55. Cobb, M.J.; Hwang, J.H.; Upton, M.P.; Chen, Y.C.; Oelschlager, B.K.; Wood, D.E.; Kimmey, M.B.; Li, X.D. Imaging of subsquamous Barrett's epithelium with ultrahigh-resolution optical coherence tomography: A histologic correlation study. *Gastrointest. Endosc.* **2010,** *71*, 223-230.

56. Lee, H.C.; Fass, O.; Ahsen, O.O.; Liang, K.; Wang, Z.; Figueiredo, M.; Potsaid, B.; Jayaraman, V.; Huang, Q.; Fujimoto, J.G.; Mashimo, H. Endoscopic optical coherence tomography microangiography identifies the altered microvasculature of the terminal ileum in Crohn's disease. *Gastrointest. Endosc.* **2017,** *85*, 511-512.

57. Luo, S.Y.; Fan, W.; Chang, H.; Liao, H.; Kang, L.; Huo. Classification of human stomach cancer using morphological feature analysis from optical coherence tomography images. *Laser Phys. Lett.* **2019**, *16*, 095602:1-9.

58. Jansen, S.M.; Almasian, M.; Wilk, L.S.; de Bruin, D.M.; van Berge Henegouwen, M.I.; Strackee, S.D.; Bloemen, P.R.; Meijer, S.L.; Gisbertz, S.S.; van Leeuwen, T.G. Feasibility of Optical Coherence Tomography (OCT) for Intra-Operative Detection of Blood Flow during Gastric Tube Reconstruction. *Sensors (Basel, Switzerland)* **2018**, *18*, 1331: 1-14.

59. Kiseleva, E.B.; Ryabkov, M.G.; Bederina, E.L.; Shirmanova, M.V.; Baleev, M.S.; Lukina, M.M.; Sirotkina, M.A.; Chilipenok, A.S.; Beschastnov, V.V.; Moiseev, A.A.; Zagaynova, E.V.; Gladkova, N.D. Observations of the bowel wall in the case of acute ischemia: optical coherence tomography, FLIM macro-imaging and histological analysis data. In Multimodal Biomedical Imaging XV, Proceedings of SPIE BiOS, 2020, San Francisco, California, United States, 17 February 2020. F.S. Azar, X. Intes, Q. Fang, Eds. SPIE: San Francisco, United States, 2020; 11232, 112320M.

60. Gelikonov, V.M.; Romashov, V.N.; Shabanov, D.V.;. Ksenofontov, S.Yu.; Terpelov, D.A.; Shilyagin, P.A.; Gelikonov, G.V.; Vitkin, I.A. Cross-polarization optical coherence tomography with active maintenance of the circular polarization of a sounding wave in a common path system. *Radiophys. Quant. El.* **2018,** *60*, 897-911.

61. Moiseev, A.; Ksenofontov, S.; Gorozhantseva, M.; Shakhova, N.; Sirotkina, M.; Kiseleva, E.; Matveev, L.; Zaytsev, V.; Zagaynova, E.; Gelikonov, V.; Gladkova, N.; Vitkin, A.; Gelikonov, G. Real time OCT-based angiography device with hand-held probe for everyday clinical use. *J Biophotonics.* **2018,** *11*, 201-217.

62. Fujimoto, J.; Swanson, E. The Development, Commercialization, and Impact of Optical Coherence Tomography. *Invest. Ophthalmol. Vis. Sci.* **2016**, *57*, OCT1–OCT13.

63. Yun, S.H.; Tearney, G.J.; De Boer, J.F.; Bouma, B.E. Motion artifacts in optical coherence tomography with frequency-domain ranging. *Opt. Express,* **2004**, *12*, 2977-2998.

64. Spaide, R.F.; Fujimoto, J.G.; Waheed, N.K. Image artifacts in optical coherence angiography. Retina (Philadelphia,Pa.), 35(11), 2163.

65. Weber, M.A., Milstein, D.M.; Ince, C.; Rengerink, K.; Roovers, JP. Vaginal microcirculation: Non-invasive anatomical examination of the micro-vessel architecture, tortuosity and capillary density. *Neurourol. Urodyn.* **2015,** *34*, 723-729.

66. Sigal, Z.M.; Surnina, O.V. A New Criterion for the Vitality of Organs is the Junction Phenomenon of the Contralateral Arterial Flows. *Int. J. Psychosocial Rehabilitation* **2020**, *24*, 240-249.

67. Furukawa A, Kanasaki S, Kono N, Wakamiya M, Tanaka T, Takahashi M, Murata K. CT diagnosis of acute mesenteric ischemia from various causes. Am J Roentgenol. 2009;192(2):408–416. doi: 10.2214/AJR.08.1138.

68. Gilbert-Kawai E, Coppel J, Bountziouka V, Ince C, Martin D; Caudwell Xtreme Everest and Xtreme Everest 2 Research Groups. A comparison of the quality of image acquisition between the incident dark field and sidestream dark field video-microscopes. BMC Med Imaging. 2016 Jan 21;16:10.

69. Ledgerwood-Lee, M.; Zifan, A.; Kunkel, D.C.; Sah, R.; Mittal, R.K. High-frequency ultrasound imaging of the anal sphincter muscles in normal subjects and patients with fecal incontinence. *Neurogastroenterol. Motil.* **2019,** *31*, 135-147.

70. Kiseleva, E.B.; Ryabkov, M.G.; Baleev, M.S.; Vorobyov, A.N.; Gelikonov, G.V.; Romanov, I.N.; Gubarkova, E.V.;. Gladkova, N.D. Intraoperative use of optical coherence angiography in ischemic bowel disease: a pilot study. In Optical and Nano-Technologies for Biology and Medicine, Proceedings of Saratov Fall Meeting, 2020, Saratov, Russian Federation, 23-27 September 2019. V. Tuchin, Ed. SPIE: 2020; 11457, 114570B.